Original Article The Eurasian Journal of Medicine EAJM 2010; 42: 47-52

The Contribution of Chemoreceptor-Network Injury to the Development of Respiratory Arrest Following Subarachnoid Hemorrhage

Subaraknoid Kanamada Nöral Kemoreseptör Yol Hasarının Solunum Arresti Gelişimine Etkisi: Deneysel Çalışma

Mehmet Dumlu Aydin[1], Atilla Eroglu[2], Atila Turkyilmaz[2], Ali Fuat Erdem[3], Hacı Ahmet Alıcı[3], Nazan Aydin[4], Sare Altas[5], Bunyami Unal[6]

Department of Neurosurgery[1], Thoracic Surgery[2], Anesthesiology and Reanimation[3], Psychiatry[4] Pathology[5] and Histology[6], Medical Faculty, Ataturk University, Erzurum, Turkey

Abstract

Objective: Respiratory arrest following brainstem herniation has been attributed to injuries resulting from compression of the respiratory centers. While it is widely perceived that the chemoreceptor network, consisting of the glossopharyngeal nerve and carotid body (GPN-CB), is essential for the modulation of respiration, its contribution to the development of respiratory arrest has not been investigated. Therefore, the aim of this study was to investigate whether injury to the GPN-CB occurs in animals with respiratory arrest caused by experimentally-induced subarachnoid hemorrhage.

Materials and Methods: Eighteen hybrid rabbits were used in this study. Four rabbits (n=4) were used to determine the normal structure of the GPN-CB. The remaining rabbits (n=14) received an autologous blood injection into the cisterna magna to produce a subarachnoid hemorrhage, after which they were observed for 20 days. The number of axons and the neuron density in the glossopharyngeal nerve and carotid body, respectively, were counted by stereological methods. The Mann-Whitney U test was used to analyze the results.

Results: Six of 14 rabbits died within the first week, likely due to brain swelling and crushing injuries that were observed in the brain stem and related structures. In control rabbits, the average neuronal density of the carotid body was 4250 ±1250/ mm^3, while the axonal density in the glossopharyngeal nerve was 18000±5100 mm^2. Conversely, in the dead rabbits, the degenerated neuron density of the carotid body was 2100±500/ mm^3, while the degenerated axon density in the glossopharyngeal nerve was 8500±2550 mm^2. In addition, histopathological lesions were more severe in the dead rabbits in terms of their glossopharyngeal nerve and carotid body.

Conclusion: There is an important relationship between neurodegeneration in the GPN-CB and mortality rates following experimentally-induced hemorrhage. This relationship suggests that injury to the GPN-CB network disrupts the breathing reflex and results in respiratory arrest following a subarachnoid hemorrhage (SAH).

Key Words: Carotid body, Glossopharyngeal nerve, Respiratory arrest, Subarachnoid hemorrhage

Özet

Amaç: Beyin sapı herniasyonu sonucu gelişen solunum arresti, respiratuvar merkezlerde olan nöronal injuriye bağlanmıştır. Kemoreseptör yolunu oluşturan glossofaringeal sinir ve karotid cisim (GPN-CB) sinir ağlarının solunum düzenlenmesindeki hayati önemi kesin bilinmesine rağmen beyin sapı patolojilerinde oluşan solunum arrestindeki rolleri henüz araştırılmamıştır. Bu çalışmanın amacı, subaraknoid kanamalarda oluşması muhtemel GPN-CB nöral devrelerdeki hasarın solunum arresti gelişimindeki etkisini araştırmaktır.

Gereç ve Yöntem: Bu çalışmada 18 hibrit tavşan incelendi. 4 tavşan GPN ve CB'nin normal yapısını belirlemek için kullanıldı. Kalan tavşanların sisterna mangalarına otolog kan verilerek subaraknoid kanama oluşturuldu ve 20 gün sonra tavşanlar incelendi. GPN'in akson sayısı ve CB'nin nöron sayısı stereolojik metotlarla hesaplandı. Sonuçlar Mann-Whitney U testi ile analiz edildi.

Bulgular: Ondört tavşanın 6'sı ilk hafta içinde öldü. Ölen hayvanların beyin sapı ve komşu yapılarında ödem ve ezilme gözlendi. Normal tavşanlarda CB'nin ortalama nöronal yoğunluğu 4250±1250/mm^3, GPN'in aksonal yoğunluğu 18000±5100/mm^2 olarak hesaplandı. Ölen tavşanlarda CB'nin dejenere nöron sayısı 2100±500/mm^3, GPN'in dejenere akson sayısı 8500±2550/mm^2 olarak hesaplandı. GPN-CB nöral ağında oluşan hasar ölen tavşanlarda daha şiddetliydi.

Sonuç: GPN ve CB'nin nörodejenerasyonu ve mortalite oranı arasında önemli bir ilişki vardır. Solunum regülasyonunda önemli bir nöral devre olan GPN-CP arkı subaraknoid kanamalarda iskemik ve mekanik hasarlara uğrayarak solunum arrestine neden olabilir.

Anahtar Kelimeler: Glossofaringeal sinir, Karotid cisim, Solunum arresti, Subaraknoid kanama

Introduction

The generation and continuation of respiration is dependent on a central driving force that consists of inspiratory and expiratory pump muscles. Respiration is modulated by neural, chemical, behavioral, voluntary, and mechanical inputs. All respiratory inputs generated by baroreceptors, chemoreceptors, pulmonary receptors, mechanoreceptors, and respiratory centers are transmitted and integrated by the somatic, sympathetic, and parasympathetic nerves [1]. Defects of the glossopharyngeal and vagus nerves can result in significant impairments in speech, swallowing, and breathing [2]. One of the most important peripheral autonomic neural pathways for respiration consists of the carotid body (CB) and glossopharyngeal nerve (GPN) [3]. The CB contains chemoreceptors that can detect hypoxia, hypercarbia, and changes in blood pH. The primary afferent neurons of the GPN then transmit information from the CB to the solitary nucleus. Some chemoreceptor afferents help mediate respiration in response to hypercarbia and hypoxia through their synaptic connections with

Received: February 19, 2010 / **Accepted:** February 25, 2010

Correspondence to: Mehmet Dumlu Aydin, Department of Neurosurgery, Medical Faculty, Ataturk University, 25240 Erzurum, Turkey
Phone: +90 442 316 63 33-2420 Gsm: +90 532 322 83 89 e-mail: nmda11@hotmail.com

doi:10.5152/eajm.2010.16

neurons in the central respiratory networks, autonomic centers, and the reticular formation [4]. Studies have shown that GPN injuries can cause severe airway obstructions and produce respiratory disturbances [5, 6]. Subarachnoid hemorrhage (SAH) can also cause respiratory arrest, which may result from severe brain edema and lesions to respiratory centers in the first days following the brain hemorrhage [7]. While injury to respiratory centers may result in respiratory arrest in SAH [8], the results from the current study indicate that SAH not only causes crushing injury to respiratory centers but also results in denervation of the CB due to radical injury to the GPN.

Materials and Methods

Eighteen hybrid rabbits that were approximately 2-years old and were 3.5 ± 0.03 kg were used in this experiment. Animal husbandry and the experimental protocol followed guidelines outlined by the National Institutes of Health, and the study design was approved by the Committee on Animal Research at Ataturk University, Erzurum, Turkey. All animals were closely monitored for electrocardiographic and respiratory irregularities. Four rabbits (n=4) were used as a control group for measuring normal cellular and axonal density in the GPN, CB and brain. The remaining rabbits (n=14) were food-deprived for 6 hours prior to surgery. Anesthesia was maintained throughout surgery to reduce pain and mortality. Anesthesia was first induced using isoflurane through a face mask, after which 0.2 mL/kg of the anesthetic combination of ketamine and xylazine (ketamine HCL, 150 mg/1.5 mL; xylazine HCL, 30 mg/1.5 mL; and distilled water, 1 mL) was subcutaneously injected. During the surgical procedure, 0.1 mL/kg of this anesthetic combination was used to maintain anesthesia. In nine animals (n=9), 0.5 mL of autologous blood was taken from the auricular artery and injected into the cisterna magna over 1 min using a 22-gauge needle. The other animals (n=5) were used as a control group (SHAM) and underwent the same procedure, but they received injections of isotonic saline. Animals were observed for 20 days without any medical treatment prior to being sacrificed. The GPN and CB were removed from all brains bilaterally and stored in 10% formalin solution for 7 days. Tissue was sectioned at 1 µm and stained using hematoxylene and eosin so that the tissue could be examined using stereological methods. Cellular shrinkage, cellular angulation, cytoplasmic condensation, and volume reduction were accepted as the criterion for neuronal degeneration in the CB. Axonal thinning and break-down were accepted as signs of axonal injury to the GPN.

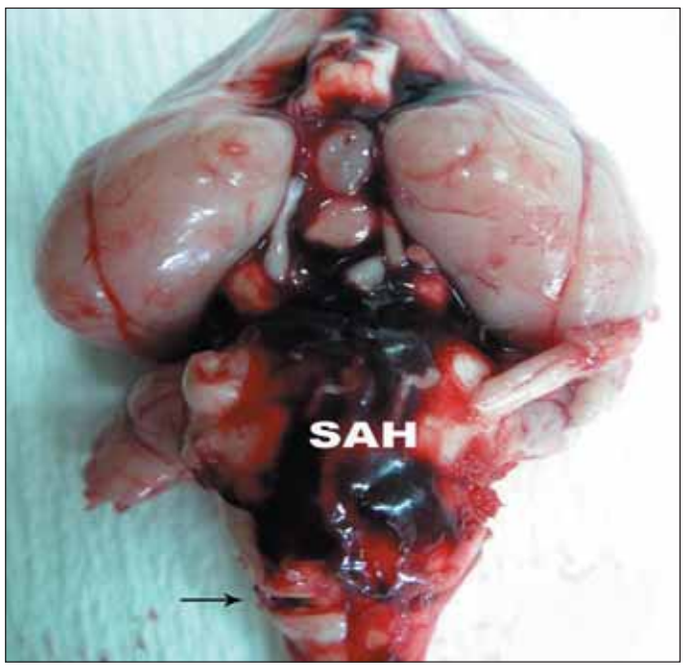

Figure 1. *Basal view of a brain with massive SAH in a deceased animal. Note the incisura of the foramen magnum in the lower medulla.*

To estimate the total number of axons in the GPN, the fractionation technique was used after the total number of cross sections from the GPN was obtained. The number was evaluated by estimating the number of axons in the GPN using an unbiased counting frame. The microscope had two attachments, a camera that transmitted information to a PC and two dial indicators with arms for mounting the microscope stage. The dial indicators (5 µm resolution) that were mounted on the microscope were capable of measuring the stage's movement in the X and Y directions. Images of the GPN cross sections were obtained according to a basic sample procedure using systematic and random stereological principles as outlined by Gundersen (1988) and were recorded with the camera. Then two unbiased counting frames of known size were mounted and sent to the PC. To estimate the mean number of normal and degenerated axons in the GPN, the axial sections of the GPN were divided into eight equal angle slices, and the number of axons in each slice were added together.

The physical dissector method was used to evaluate the number of neurons in the CB. This method has several advantages in that it 1) easily estimates the number of particles, 2) is both readily performed and intuitive, 3) does not make assumptions about the particle shape, size and orientation, and 4) is unaffected by overprotection and truncation. Two consecutive sections (dissector pairs) were obtained from tissue samples with named references and were mounted on each slide. Reference and look-up sections were reversed to double the number of dissector pairs without taking new sections. The mean numerical density of normal and degenerated neurons (per mm^3) in the CB (NvGN) were estimated using the following formula, where SQ-N is the total number of counted neurons appearing only in the reference sections, t is the section thickness, and A is the area of the counting frame:

$$NvGN = SQ\text{-}N/txA$$

The Cavalieri volume estimation method was used to obtain the total number of neurons in each specimen. The total number of neurons was calculated by multiplying the volume (mm^3) and the numerical density of neurons in the CB. The number of living and degenerated neurons in the GPN and CB of all animals was counted. Data analysis was performed using the Mann-Whitney U test.

Results

Six animals in the experimental group (n=6) and two animals in the SHAM group (n=2) were dead within the first week after surgery. Neck stiffness, unconsciousness, convulsive attacks, fever, apnea, cardiac arrhythmia, and breathing disturbances were observed in all dead animals.

In control animals, the heart rate was 260±25/min, the respiratory rate was 33±8/min and the blood oxygen concentration was 90±5%. Soon after inducing SAH, the heart rate decreased to 140±40/min,

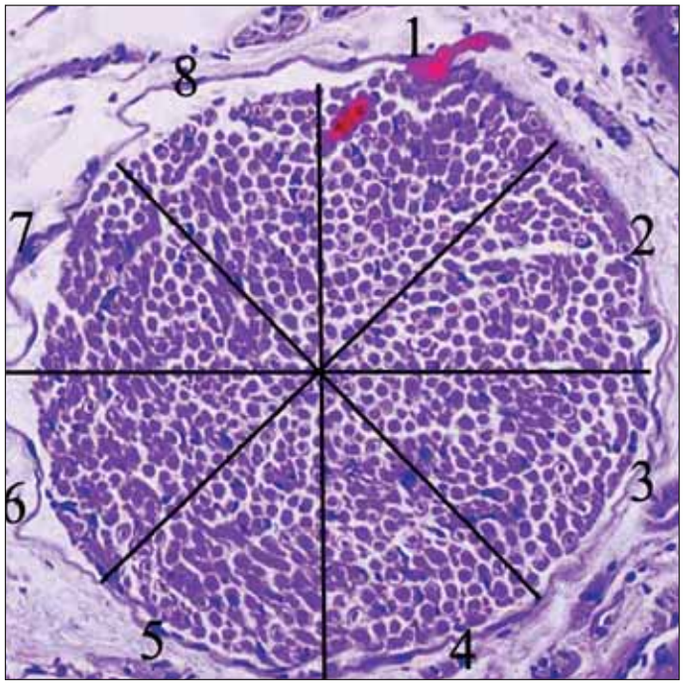

Figure 2. *Histopathological appearance of GPN axons in a normal rabbit. To estimate the mean number of GPN axons, an axial section of the GPN was divided into eight equal angle slices, and the number of axons in each slice was summed together (GPN, LM, H&E, x 40).*

the respiratory rate was 17±6/min, and the blood oxygen concentration was 75±10%. Considerable electrocardiographic changes were observed such as ST depression, ventricular extrasystoles, bigeminal pulses, QRS separation, and fibrillations. However, in the late phase of fatality-inducing SAH, the heart rate increased to 330±30/min. When analyzing respiratory parameters, both decreased respiration frequency (bradipne) (17±6) and increased respiratory amplitudes (35%) were observed in the first hours following SAH. However, at longer intervals following SAH, increased respiration frequency (tachipne) and decreased respiration amplitude (32±8%) were observed, resulting in shortened inspiration, a longer expiration time, apne-tachypnea attacks, diaphragmatic breath and respiratory arrest (10±4).

An example of the gross pathologic appearance of brains from rabbits that died from massive SAH is given in Figure 1. These brains had swelling and compression of the foramen magnum in the lower medulla. The method for assessing axon numbers is shown in Figure 2, while the normal histological appearance of the GPN has been magnified in Figure 3. Axonal swelling, periaxonal thinning, axonal loss, and interaxonal vacuolizations were used as the criteria for determining axonal degeneration (Figure 4). The numerical density of normal axons in the GPN was 18000±5100 mm^{-2} in normal rabbits and 16200±1500 mm^{-2} in surviving animals. The number of live axons was 12500±3650 axon/mm^2 in the surviving animals, but there were only 8500±2250 axon/mm^2 live axons in the dead animals. Hence, the number of live axons in the GPN of surviving animals was significantly higher than those found in the dead animals ($p<0.005$). Similarly, there were significantly fewer degenerated axons in the surviving animals than in the dead animals ($p<0.001$).

The mean total volume of the CB was calculated to be 0.8±0.2 mm^3. The histological appearance of normal neurons in the CB and the number of neurons in the CB (estimated using physical dissector pairs) are presented in Figure 5 A-B. Using histopathological examination, the criteria for neuronal degeneration in CB neurons in deceased animals was cytoplasmic condensation, nuclear shrinking, cellular angulations, and peri-cytoplasmic halo formation secondary to cytoplasmic regression (Figure 6). The mean neuronal numerical density in the CB was 4250±1250 mm^{-3}. In the surviving animals, a majority of CB neurons were living (4000±750), and the numerical density of degenerated neurons was 250±50. However, in the dead animals, a large number of CB neurons were degenerated (2100±500), and the numerical density of living CB neurons was only 2300±250. Hence, relative to the surviving animals, dead animals had significantly more degenerated neurons ($p<0.0001$) and significantly fewer live neurons ($p<0.001$). Table 1 shows the mean number of live and degenerated neurons in the CB of both the surviving and dead animals.

Table 1. The average live and degenerated neuron density (neuron numbers/mm^3) in the CB of normal, surviving, and dead rabbits. The difference in the number of degenerated neurons between the dead and surviving animals was significant ($p<0.0001$) (CB: Carotid Body)

	Live	Degenerated
Normal	4250±1250	10±3
Living animals	4000±150	250±50
Dead animals	2300±250	2300±450

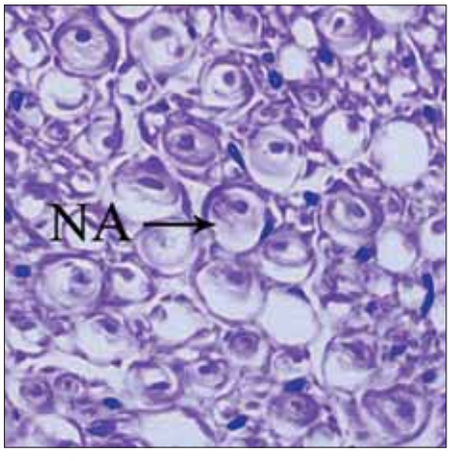

Figure 3

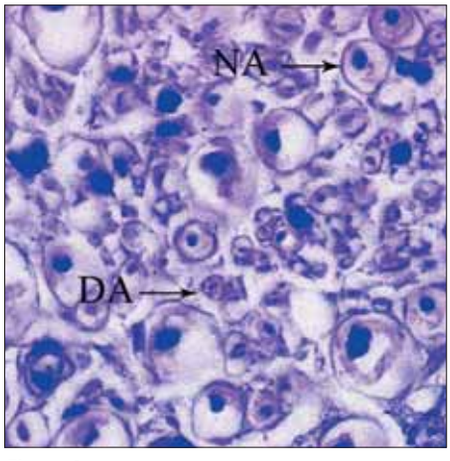

Figure 4

Figure 3. *Normal axons (NA) in the GPN shown under magnification (LM, H&E, x100).*

Figure 4. *Normal axons (NA) and degenerated axons (DA) in the GPN of animals that died following SAH, shown under magnification (LM, H&E, x100).*

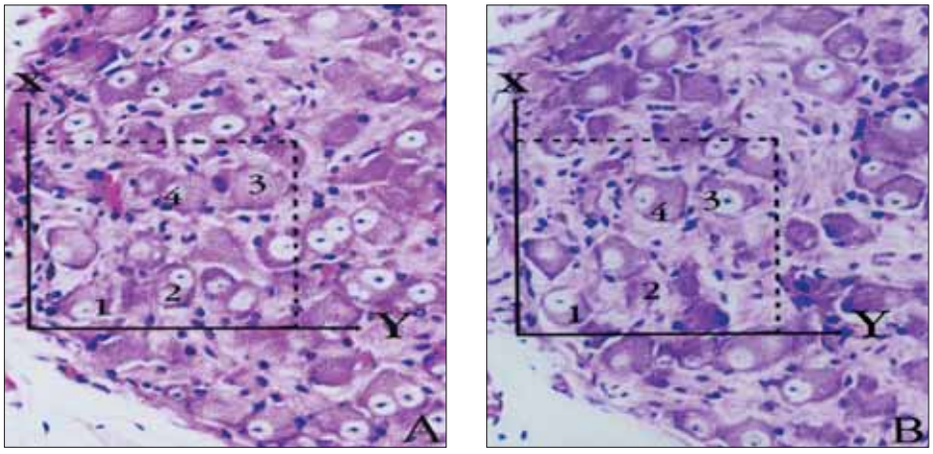

Figure 5 (A-B). *NPhysical dissector pairs of carotid bodies seen in rabbits. In the application of the physical dissector method, micrographs in the same fields of view (a,b) are taken from two parallel, adjacent thin sections separated by a distance of 5 mm. The upper and right lines of an unbiased counting frame represent the inclusion lines, while the lower and left lines (including the extensions) represent the exclusion lines. Any neuron nucleolus hitting the inclusion lines is excluded, while nucleolus profiles that hit the inclusion lines and are located inside the frame are counted as dissector particles unless their profile extends into the look-up section. The neurons from the two dissectors have a volume calculated by taking the product of the counting frame and the distance between the sections. The numerical neuron density is calculated by the equation, NvGN = ΣQ–GN/txA. In this application, the nucleoli marked with '1,4' are dissector particles. In contrast, nucleoli marked with '2,3' are not dissector particles in section A because they disappeared in section B (H&E, 200, LM).*

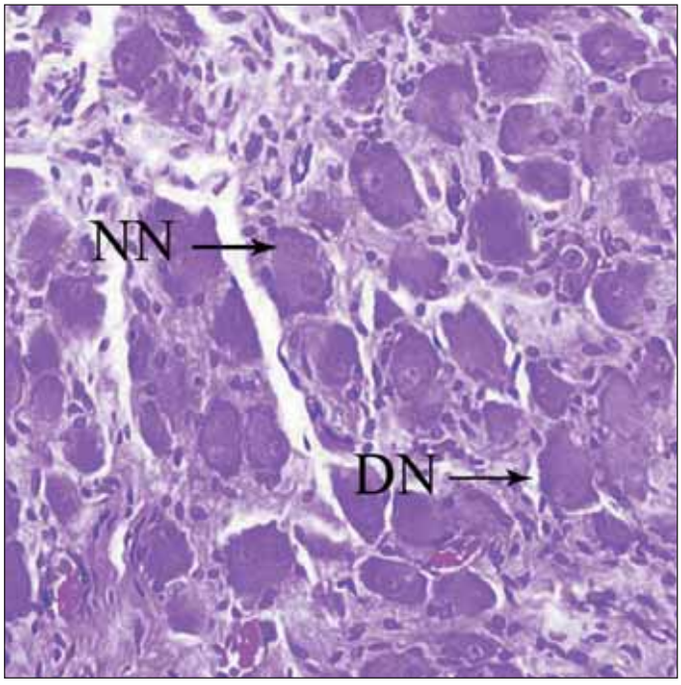

Figure 6. *A magnified histopathological image of the CB from a dead animal. Cytoplasmic condensation, nuclear shrinking, angulation, and peristoplasmic halo formation were all observed in this tissue (NN, Normal Neuron; DN, Degenerated neuron), (LM, H & E, x 100, LM).*

Table 2. The estimated numerical density of GPN axons (axon density/mm²) in each group. There were significant differences in the number of degenerated axons between the living and dead animals (P<0.001)

	Live	Degenerated
Normal (Axon density mm^{-2})	18000±5100	10±2
Living animals	16200±1500	1650±750
Dead animals	9500±3650	8500±2550

Table 3. The average degenerated axon density (DA/mm³) in the GPN and the respiratory frequency (f/minute) in normal, surviving, and dead rabbits. The differences in the number of degenerated axons in GPN as well as the respiratory frequency were significantly different in dead animals relative to surviving animals (p<0.0001)

	DA/mm^3	f/minute
Normal	10±2	33±8
Living animals	1650±750	28±7
Dead animals	8500±3650	10±4

In addition, there were significant differences between groups in the number of degenerated axons in the GPN and the number of degenerated neurons in the CB (p<0.0001). Table 2 shows the mean number of live and degenerated axons in the GPN as well as the number of CB neurons in both the surviving and dead animals.

Lastly, there were significant differences between groups when comparing the number of degenerated axons in the GPN, the number of degenerated CB neurons, and the frequency of respiratory rhythm irregularities (p<0.0001) (Table 3).

Discussion

The generation and modulation of respiration is dependent on a central driving force consisting of inspiratory and expiratory pump muscles. Importantly, respiration can be modulated by many chemical, mechanical, and neural inputs. Autonomic control of respiration depends on peripheral sensors, including arterial baroreceptors and chemoreceptors, pulmonary and muscular mechanoreceptors, and afferent and efferent autonomic pathways. Respiratory functions can also be affected by the endocrine system, behavioral and voluntary states, and various molecular factors [9]. The neural network responsible for chemoreception consists of the GPN and CB. The GPN and vagal nerves are responsible for carrying all of the sensory afferent fibers, including those from baroreceptors, chemoreceptors, and pulmonary receptors. Respiratory afferents first interact in the solitary nucleus before subsequently interacting in the respiratory nucleus of the brainstem. The efferent inputs that are necessary to maintain continuous functioning of the respiratory system include the GPN, vagal nerve, sympathetic nerves, somatosensitive nerves, and somatomotor nerves. The viscerosensitive nerve endings of the GPN and vagal nerves are important for initiating breathing reflexes and regulating autonomic control over respiration [1]. The basic neural circuitry of the CB consists of relays between itself, the GPN, and the respiratory center complex, the latter of which consists of the pneumotaxic, apneustic, inspiratory, and expiratory nucleus of

the brain stem [5]. Peripheral chemoreceptors in the CB detect minor changes in oxygen and carbon dioxide-hydrogen levels in the bloodstream. In the GPN, the primary afferent nerve terminals extend from the petrosal ganglia to transmit information to the solitary nucleus of the brain stem. The primary chemoreceptor afferents from the petrosal ganglia synapse with parasympathetic and presympathetic neurons in the brain stem and, as a result, can mediate cardiovascular responses to hypercarbia and hypoxia. Ischemia in the lower brain stem produces concomitant changes in tissue oxygen, carbon dioxide partial pressures, and acidosis, thereby causing intense vasoconstriction and increased ventilation [4]. Chemoreceptors located close to the ventral surface of the medulla respond to changes in CO2 and pH levels of the cerebrospinal fluid. Chemical information coming from the surface areas of the medulla are integrated with information from the CB at respiratory centers [9]. In this situation, the sensitivity of the chemoreceptors can change, producing a chaotic state at centers that regulate pH of the body.

SAH is defined as blood leakage in the subarachnoid space, cisterns, and sometimes in the brain ventricles. SAH can be experimentally-induced by injecting autologous blood into the cisterna manga, which creates pathological processes highly similar to those of spontaneous SAH. Vasospasm and disrupted cerebral autoregulation are the most serious problems during the progression of SAH. Severe SAH can produce loss of cerebral autoregulation, while microvascular aggregation of red blood cells may also cause acute ischemic damage [10, 11]. As SAH progresses, ischemia may be worsened by the swelling of the perivascular astrocytes and neurons, endothelin-induced ischemic insult, and increased cerebrovascular resistance [12]. High blood pressure may create an even more severe outcomes following SAH [13]. The mortality rate following SAH is about 25% within 24 hours and 45% within 30 days due to lower brain herniation [14]. A profound elevation in intracranial pressure is an important factor in the development of brain herniation [15]. While decreases in cerebral blood flow and cerebral perfusion pressure are significant factors contributing to early mortality [15], injury to the CB peripheral network is also an important concern.

The CB contains the main arterial chemoreceptors, which are characterized by having high blood flow, an elevated metabolism, and oxygen-sensing functions and being susceptible to damage following changes in arterial blood pH. They also have a vital role in mediating cerebrovascular and respiratory autoregulation. As a result, vasoactive molecules produced by the CB may modulate chemosensory processes by controlling CB blood flow and tissue PO2. Chemosensitive units in the CB are glomoid structures comprised of glomus cells clustered around the capillaries. Glomus cells are synaptically connected to nerve terminals of the petrosal ganglion neurons via the GPN [16]. Glomus cells respond to hypoxia, hypercapnia, and acidosis by releasing appropriate transmitters and creating a chemosensory discharge that stimulates the sensory petrosal ganglion neurons [17].

The CB undergoes significant morphological and functional changes following alterations in oxygen concentration [18] as well as hypoxia-induced glomus cell secretion. However, its ability to respond to such changes decreases with age [19]. The expanded vasculature in a chronically-hypoxic CB returns to the normoxic control state in early-ending hypoxia approximately 8 weeks after the termination of hypoxia [20, 21]. Chronic hypoxia causes enlargement, hyperplasia, and neo-vascularization of the CB [3]. In addition, high altitudes and decreased oxygen pressure can also cause the CB to exhibit increased activation of the afferent nerves [22]. CB dysfunction can also result in failure or arrest of cerebrovascular and respiratory autoregulation [7]. The baroreflex failure syndrome occurs after the bilateral excision of the CB [23]. Baroreceptor denervation results in temporary or permanent increases in blood pressure [24]. CB tumor resection and neck irradiation result in severe hypertension and tachycardia attacks [25]. Recovery from neuronal damage to the CB following ischemia may be facilitated via early revascularization of the CB by posterior cerebral circulation [26]. It has been postulated that neuronal deterioration or functional deficiencies of the CB can actually worsen a patient's prognosis following SAH. Brief periods of fetal hypoxia have been shown to produce neuronal death in the cerebellum, hippocampus, and cerebral cortex and can actually cause death stemming from tonsillar herniation [27]. Over time, CB degeneration occurs and chemoreflex mechanisms are destroyed [28]. Cholinergic inputs from both the hypothalamus and CB to the GPN are activated by hypotension [29].

Foramen magnum lesions are an important cause of acute respiratory insufficiency. Both cerebellar ectopia and syringomyelia may have symptoms including progressive nocturnal hypoventilation, obstructive sleep apnea, and sometimes sudden respiratory arrest [30]. In Chiary Type I, compression of the GPN by the cerebellar tonsils may cause cardiac syncope given that symptoms disappear after surgical treatment [31]. Ultrastructural and histopathological changes have been reported in denervated CB neurons [32]. The carotid branch of the GPN transsection can lead to severe CB degeneration [33]. Despite the hypothalamus' important role in modulating cardio-respiratory reflexes, it fails to affect the CB in animals with denervated neurons [5]. GPN injuries can cause severe obstruction of the airways due to pharyngeal muscle paralysis, hypertension, and respiration disorders [6]. Evidence has suggested that the herniated brain may cause compression of the GPN rootlets and vasa nervorum, thereby leading to GPN damage. GPN injury may result in CB denervation and atrophy such that respiratory reflexes are subsequently disrupted.

The present study principally assessed the relationship between degenerated GPN axons and CB neurons in animals that either survived or died following SAH. The methods used to estimate the number of live and degenerated GPN axons and CB neurons were of an important consideration. Because previous counting methods have been shown to be biased, we chose to use stereological methods for these calculations. Stereology is a superior mathematical method for abstracting three-dimensional measurements from two-dimensional structures and for dealing with quantitative factors such as shape, size, number, and orientation in space [8, 34, 35].

According to our stereological analyses, neurodegenerative changes in the GPN and CB were more evident in cases where the SAH treatment was fatal. The differences between the number of broken axons in the GPN and the number of degenerated neurons in the CB were less robust in the surviving animals ($p<0.005$) than in animals that had fatalities ($p< 0.0001$).

Brain-stem herniation is known to be one of the most important factors in both the etiology of respiratory disturbances and sudden death in neurosurgical practices. According to current research, neurochemical pathways including the GPN and CB have an important role in regulation of respiratory rhythm, maintenance of blood flow, and cerebral autoregulation. Even though damaged respiratory

centers can cause respiratory arrest during brain-stem herniation, the histopathological changes that occur in the GPN and CB have not previously been investigated. The present experimental results indicate that brain-stem herniation can crush the GPN and blood vessels, resulting in injury to the GPN and CB. Therefore, crushing injuries of the GPN and CB may be a likely cause of respiratory arrest in fatal SAH.

In summary, a herniated brain stem may compress the GPN and related vascular units, thereby causing GPN damage and denervation atrophy of CB neurons. As a result, mechanical, chemical, sensitive, and autonomic impulses that are critical for stimulating respiration cannot be transmitted to respiratory regulating centers. Because normal respiration is impossible in brain stem pathologies due to upper respiratory muscles paralysis, respiratory arrest may be inevitable as SAH progresses. GPN-CB network injury should be taken into consideration as a cause of respiratory arrest, and new treatments should be investigated to prevent injury to the GPN-CB in these situations.

Conflict of interest statement: The authors declare that they have no conflict of interest to the publication of this article.

References

1. Coleridge HM, Coleridge JCG, Jordan D. Integrations of ventilatory and cardiovscular control systems. In Crystal RG & West JB eds. The Lung, New York, Raven Pres Scientific Foundations 1991; 1405-18.
2. Erman AB, Kejner AE, Hogikyan ND, et al. Disorders of cranial nerves IX and X. Semin Neurol 2009; 29: 85-92.
3. Prabhakar NR, Jacono FJ. Cellular and molecular mechanisms associated with carotid body adaptations to chronic hypoxia. High Alt Med Biol 2005; 6: 112-20.
4. Guyenet PG. Neural structures that mediate sympathoexcitation during hypoxia. Respir Physiol 2000; 121: 147-62.
5. Reddy MK, Patel KP, Schultz HD. Differential role of the paraventricular nucleus of the hypothalamus in modulating the sympathoexcitatory component of peripheral and central chemoreflexes. Am J Physiol Regul Integr Comp Physiol 2005; 289: 789-97.
6. Hanamori T, Kunitake T, Kato K, et al. Fiber types of the lingual branch of the trigeminal nerve, chorda tympani, lingual-tonsillar and pharyngeal branches of the GPN, and superior laryngeal nerve and their relation to the cardiovascular responses in rats. Neurosci Lett 1996; 219: 49-52.
7. Doux JD, Yun AJ. The link between carotid artery disease and ischemic stroke may be partially attributable to autonomic dysfunction and failure of cerebrovascular autoregulation triggered by Darwinian maladaptation of the carotid baroreceptors and chemoreceptors. Med Hypotheses 2006; 66: 176-81.
8. Gundersen HJ, Bendtsen TF, Korbo L, et al. Some new, simple and efficient stereological methods and their use in pathological research and diagnosis. APMI 1988; 96: 379-94.
9. Berger AJ, Mitchel RA, Severinghouse JW. Regulation of respiration. New England Journal of Medicine 1977; 297: 92-7.
10. Berger AJ, Mitchell RA, Severinghaus JW. Cortical blood flow and cerebral perfusion pressure in a new noncraniotomy model of subarachnoid hemorrhage in the rat. Stroke 1995; 26: 1086-91.
11. Jakobsen M. Role of initial brain ischemia in subarachnoid hemorrhage following aneurysm rupture: A pathophysiologic survey. Acta Neurol Scand 1992; 141: 1-33.
12. Ames A, Wright RL, Kowada M, et al. Cerebral ischemia. II. The no-reflow phenomenon. Am J Pathol 1968; 52: 437-53.
13. Oikawa S, Hirakawa H, Kusakabe T, et al. Autonomic cardiovascular responses to hypercapnia in conscious rats: the roles of the chemo- and baroreceptors. Auton Neurosci 2005; 117: 105-14.
14. Broderick JP, Brott TG, Duldner JE, et al. Initial and recurrent bleeding are the major causes of death following subarachnoid hemorrhage. Stroke 1994; 25: 1342-7.
15. Bederson JB, Levy AL, Ding WH, et al. Acute vasoconstriction after subarachnoid hemorrhage. Neurosurgery 1998; 42: 352-60.
16. Schultz HD, Sun SY. Chemoreflex function in heart failure. Heart Fail Rev 2000; 5: 45-56.
17. Rey S, Iturriaga R. Endothelins and nitric oxide: vasoactive modulators of carotid body chemoreception. Curr Neurovasc Res 2004; 1: 465-73.
18. Wang ZY, Bisgard GE. Postnatal growth of the carotid body. Respir Physiol Neurobiol 2005; 149: 181-90.
19. Donnelly DF. Development of carotid body/petrosal ganglion response to hypoxia. Respir Physiol Neurobiol 2005; 149: 191-9.
20. Kusakabe T, Hirakawa H, Oikawa S, et al. Morphological changes in the rat carotid body 1, 2, 4, and 8 weeks after the termination of chronically hypocapnic hypoxia. Histol Histopathol 2004; 19: 1133-40.
21. Kusakabe T, Matsuda H, Hayashida Y. Hypoxic adaptation of the rat carotid body. Histol Histopathol 2005; 20: 987-97.
22. Wilson DF, Roy A, Lahiri S. Immediate and long-term responses of the carotid body to high altitude. High Alt Med Biol 2005; 6: 97-111.
23. De Toma G, Nicolanti V, Plocco M, et al. Baroreflex failure syndrome after bilateral excision of carotid body tumors: an underestimated problem. J Vasc Surg 2000; 31: 806-10.
24. Timmers HJ, Wieling W, Karemaker JM, et al. Baroreflex failure: a neglected type of secondary hypertension. Neth J Med 2004; 62: 151-5.
25. Timmers HJ, Wieling W, Karemaker JM, et al. Cardiovascular responses to stress after carotid baroreceptor denervation in humans. Ann N Y Acad Sci 2004; 1018: 515-9.
26. Aydin MD, Ozkan U, Gundogdu C, et al. Protective effect of posterior cerebral circulation on carotid body ischemia. Acta Neurochir 2002; 144: 369-72.
27. Rees S, Inder T. Fetal and neonatal origins of altered brain development. Early Hum Dev 2005; 81: 753-61.
28. Pokorski M, Walski M, Dymecka A, et al. The aging carotid body. J Physiol Pharmacol 2004; 3: 107-13.
29. Silveira SA, Viana Lima NR, Haibara AS, et al. The hypothalamic paraventricular nucleus and carotid receptors modulate hyperglycemia induced by hemorrhage. Brain Res 2003; 993: 183-91.
30. Fish DR, Howard DS, Wiles CM, et al. Respiratoy arrest. A complication of cerebellar ectopia in adults. Journal of Neurol Neurosurg Psychiatry 1988; 51: 714-7.
31. Aguiar PH, Tella OI Jr, Pereira CU, et al. Chiari type I presenting as left glossopharyngeal neuralgia with cardiac syncope. Neurosurg Rev 2002; 25: 99-102.
32. Abbott CP, De Burgh, Daly M, et al. Early ultrastructural changes in the carotid body after degenerative section of the carotid sinus nerve in the cat. Acta Anat 1972; 83: 161-85.
33. Pequignot JM, Hellström S, Forsgren S, et al. Transection of carotid sinus nerve inhibits the turnover of dopamine and norepinephrine in long-term hypoxic carotid bodies: a biochemical and morphometric study. J Auton Nerv Syst 1991; 32: 165-76.
34. Sterio DC. The unbiased estimation of number and sizes of arbitrary particles using the disector. J Microsc 1984; 134: 127-36.
35. Cruz-Orive LM, Weibel ER. Recent stereological methods for cell biology: a brief survey. Am J Physiol 1990; 258: 148–56.